Contents lists available at ScienceDirect

Transactions of Nonferrous Metals Society of China

36(2026) 171−182

www.tnmsc.cn

Effect and mechanism of Ti−O solid solution layer on interfacial bonding strength of cold roll bonded titanium/stainless steel laminated composite plate

Zhi-yan YANG [a,b,c], Xue-feng LIU [a,b,c,*], Hong-ting CHEN [a,b,c], Xin MA [a,d]

[a] Beijing Advanced Innovation Center for Materials Genome Engineering, University of Science and Technology Beijing, Beijing 100083, China;

[b] Beijing Laboratory of Metallic Materials and Processing for Modern Transportation, University of Science and Technology Beijing, Beijing 100083, China;

[c] Key Laboratory for Advanced Materials Processing of Ministry of Education, University of Science and Technology Beijing, Beijing 100083, China;

[d] School of Mechanical and Electrical Engineering, Xinjiang Institute of Engineering, Urumqi 830023, China

Abstract: Titanium plates with a Ti−O solid solution surface-hardened layer were cold roll-bonded with 304 stainless steel plates with high work hardening rates. The evolution and mechanisms affecting the interfacial bonding strength in titanium/stainless steel laminated composites were investigated. Results indicate that the hardened layer reduces the interfacial bonding strength from over 261 MPa to less than 204 MPa. During the cold roll-bonding process, the hardened layer fractures, leading to the formation of multi-scale cracks that are difficult for the stainless steel to fill. This not only hinders the development of an interlocking interface but also leads to the presence of numerous microcracks and hardened blocks along the nearly straight interface, consequently weakening the interfacial bonding strength. In metals with high work hardening rates, the conventional approach of enhancing interface interlocking and improving interfacial bonding strength by using a surface-hardened layer becomes less effective.

Keywords: titanium/stainless steel laminated composite plate; Ti−O solid solution hardened layer; interlocking interface formation mechanism; interfacial bonding strength

1 Introduction

The interfacial bonding strength is a critical mechanical property of laminated metal composites [1]. Due to the complexity of the interface bonding process, the evolution of the interface structure morphology and its impact on the interfacial bonding strength are not yet fully understood. The cold roll bonding method, with its low production cost, high efficiency, and simplicity, is a primary method for preparing laminated metal composites. Researchers have conducted extensive research on the factors influencing and controlling the interfacial bonding strength at cold roll bond interfaces [2−4].

It is recognized that a hardened layer, susceptible to rupture due to deformation, present on the surface intended for bonding, will rupture during the cold roll bonding process. This rupture allows the component metals to flow, filling the cracks and embedding the fragments of the hardened layer, easily forming an interlock morphology at the bond interface and thereby

Corresponding author: *Xue-feng LIU, Tel: +86-10-62333627, E-mail: liuxuefengbj@163.com

https://doi.org/10.1016/S1003-6326(25)66956-1

Received 28 April 2024; accepted 10 January 2025

enhancing the interfacial bonding strength [5−7]. The rupture of the hardened layer during cold roll bonding exposes fresh virgin metal at the interface, which simplifies the bonding process [8]. Consequently, forming a hardened layer on the surface intended for bonding has become an effective method to enhance the bonding strength at the cold roll bond interface. For instance, WU et al [9] developed a nitrogen-enriched hardened layer on the steel plate intended for bonding. When the steel plate is cold roll bonded with the aluminum plate, the relatively low-strength aluminum extrudes to fill the cracks in the hardened layer, promoting significant crack expansion. The nitrogen-enriched hardened fragments drive the steel substrate to embed deeply into the aluminum side, forming a multiscale strongly interlocked interface between aluminum and steel, which significantly enhances the interfacial bonding strength.

However, FAKHER et al [10] provide new insights into how a hardened layer on the bonding surface affects interfacial bonding strength in cold roll bonding. In their study, they cold-roll-bonded a pure aluminum sheet with a chromium hardened layer on its bonding surface to another pure aluminum sheet with identical mechanical properties. They found that it was more difficult to extrude virgin metal into the cracks of the chromium hardened layer at the aluminum/aluminum interface. As a result, the area of virgin metal bonding decreased, leading to a reduction in interfacial bonding strength. Thus, besides the hardened layer on the bonding surface, the strength difference between the component metals is also a crucial factor affecting interfacial interlock [11]. It can also be reasonably predicted that changes in the strength of the component metals during the cold roll bonding process will affect interfacial interlock. The strength of metals during deformation is primarily determined by their work-hardening rate, and it is expected that when the component metals exhibit a high work-hardening rate, the strength of the component metals rapidly increases, resulting in significantly different interfacial interlock behavior. However, there have been few studies examining the effect of hardened layers on interlocking behavior and interfacial bonding strength in cold roll-bonded interfaces with component metals that have high work-hardening rates.

Titanium/stainless steel laminated composite plates (TSSLCP) combine the excellent corrosion resistance of titanium with the excellent mechanical properties of stainless steel [12,13], with broad application prospects in the petrochemical, marine, aerospace, and other industries. Cold deformation of 304 stainless steel results in deformation-induced martensitic phase transformation and a high work-hardening rate [14,15]. This study investigates the changes in interfacial bonding strength and the underlying mechanisms in TSSLCP, using TA2 titanium plate and 304 stainless steel plate as raw materials. Before cold roll bonding with stainless steel, a hardened layer is created on the surface of the titanium plate. The objective of this study is to deepen our understanding of the interfacial bonding process and provide theoretical support for the development of the metal laminated composite materials with superior interfacial bonding strength.

2 Experimental

2.1 Preparation of TSSLCP

Under high-temperature conditions, titanium readily absorbs oxygen on its surface, forming a Ti−O solid solution layer with high hardness that is prone to rupture during deformation [16,17]. This layer can reach thicknesses of up to tens of micrometers. The advantage of the Ti−O solid solution layer is that it is in-situ generated and easily obtainable, with adjustable thickness over a wide range. It serves as a cost-effective alternative for the hardening layer on the bonding surface.

The raw materials used in this study were 1.5 mm-thick commercial cold-rolled TA2 titanium sheets and 304 stainless steel sheets. The preparation process for TSSLCP was as follows:

(1) The titanium and stainless steel plates were annealed for 30 min and then pickled to remove the oxide film from their surfaces. The titanium plates were annealed at 800 and 1000 °C to produce Ti−O solid solution layers with varying thicknesses. The morphology of these layers is consistent with previous reports in the literature [16,18], as shown in Fig. 1. The thickness of the Ti−O solid solution layer increases from approximately 15 to 25 μm as the annealing temperature of the titanium plate rises from 800 to 1000 °C. Additionally, the stainless steel plate was annealed at 1050 °C to reduce its initial deformation resistance.

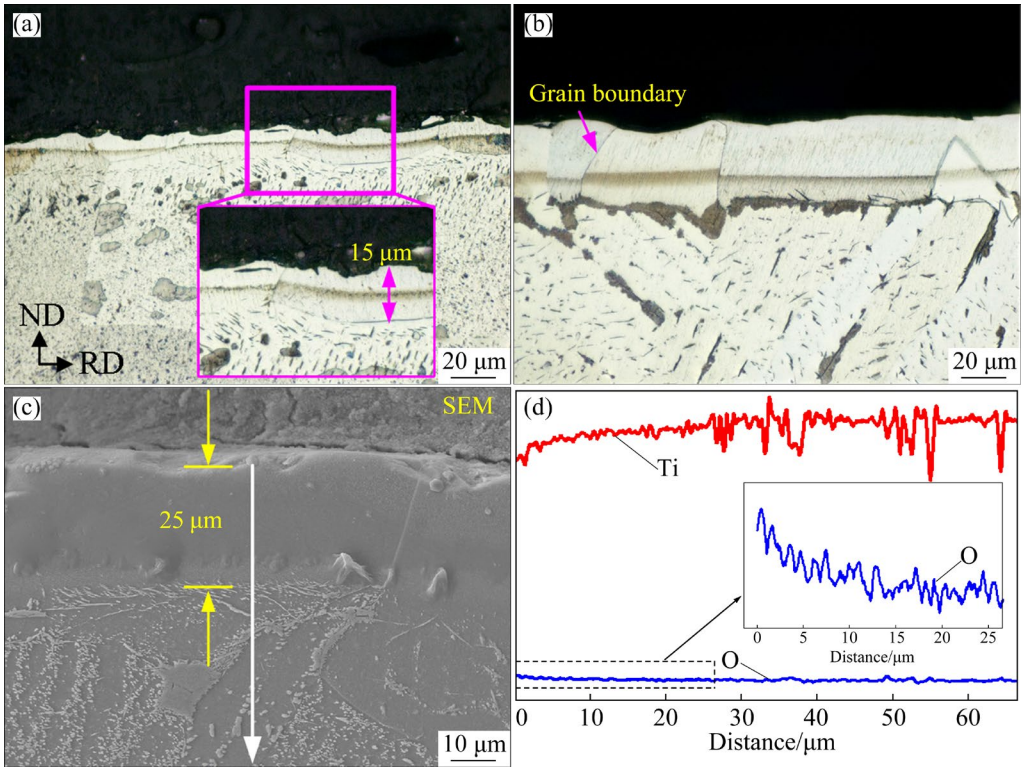

Fig. 1 Effect of annealing temperature on thickness of Ti−O solid solution layer: (a) 800 °C; (b, c) 1000 °C; (d) Elemental composition at position of white arrow in (c)

(2) The bonding surface was ground using an angle grinder with diamond blades to remove contaminants. During grinding, a micrometer was used to roughly measure the amount of material removed from the bonding surface of titanium plate. The removal amounts were set to be 5 and 50 μm to control the thickness of the Ti−O solid solution layer in the designated bonding area of the titanium plate.

(3) The ground titanium and stainless steel plates were laminated into a billet and fed into a four-roll cold rolling mill for two passes of cold roll bonding, with reduction of 50% and 30% for each pass, to achieve the cold-rolled state of the TSSLCP. During this process, the working rolls of the cold rolling mill had a diameter of 110 mm, and the rolling speed was 0.04 m/s.

(4) The cold-rolled TSSLCP was placed into a small box resistance furnace and then subjected to diffusion annealing at 600 °C for 10 min, followed by air cooling to room temperature. The annealing temperature and duration were based on Refs. [19, 20], ensuring that the TSSLCP bond interface did not overreact and that the titanium component layer could fully recrystallize.

2.2 Mechanical properties testing and microstructure characterization

In accordance with the standard GB/T 6396—2008, tensile-shear tests were conducted on a WDW−200D universal testing machine to evaluate interfacial bonding strength of TSSLCP. Figure 2 shows a schematic diagram of the tensile-shear specimen, with the crosshead moving at a rate of 1 mm/min. The average value was determined from three specimens per group. The hardness of the TSSLCP bond interface in its cold-rolled state was measured using a Vickers hardness tester.

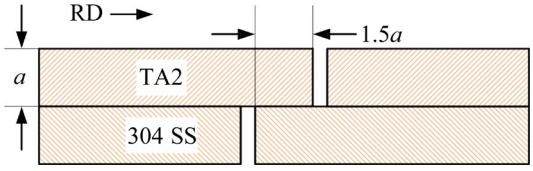

Fig. 2 Schematic diagram of tensile-shear specimen

The phase composition of the peel interface of the cold-rolled TSSLCP was analyzed using an X-ray diffractometer (XRD-SmartLab) over a scanning range of 30°−100° and at a scanning speed of 10 (°)/min. A field-emission scanning electron microscope (SEM-Zeiss Gemini 500) equipped

with an energy-dispersive spectrometer (EDS-ULTIM MAX) was used to observe the microstructure and perform elemental analysis of the specimens. The microstructure of the RD−ND cross-section of the TSSLCP was characterized using an EBSD analysis system integrated with an SEM. The EBSD samples were prepared using a combination of mechanical polishing and argon ion milling. The EBSD data, collected at a step size of 0.06 μm, were processed using Channel 5 software. The titanium plates were etched using a modified Kroll's reagent, which consisted of 60 mL H_2O, 3.5 mL HF, 1 mL HNO_3, and 1 g MgF_2, and their structure morphology was observed under a metallographic microscope (Olympus BX53).

3 Results

3.1 Mechanical properties of bond interface

Figure 3 illustrates the influence of the annealing process on titanium plates, as well as the thickness of the Ti−O solid solution layer, on the interfacial bonding strength of TSSLCP. Figure 3 shows that when a Ti−O solid solution layer is present on the bonding surface, the interfacial bonding strength of TSSLCP decreases from 204 to 163 MPa as the layer thickness increases from approximately 10 to 20 μm. Conversely, the absence of the Ti−O solid solution layer on the bonding surface leads to a significant increase in the interfacial bonding strength of TSSLCP. Furthermore, annealing the titanium plates at 800 and 1000 °C results in interfacial bonding strengths of 271 and 261 MPa for TSSLCP, respectively. In this experiment, the presence of the Ti−O solid solution layer on the bonding surface has the most significant impact on the interfacial bonding strength, leading to a reduction, while the annealing temperature of titanium plates has comparatively less effect.

Figure 4 shows the hardness of the TSSLCP bond interface in its cold-rolled state, highlighting

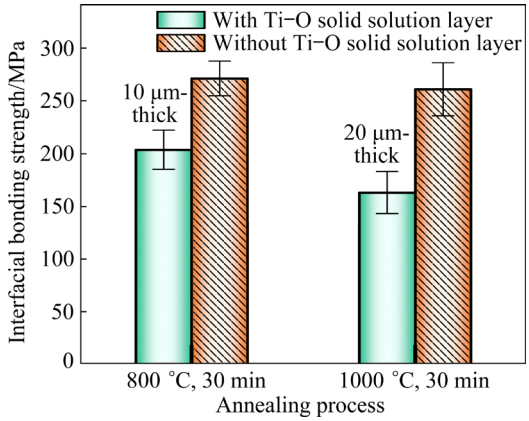

Fig. 3 Effect of annealing titanium plates on interfacial bonding strength

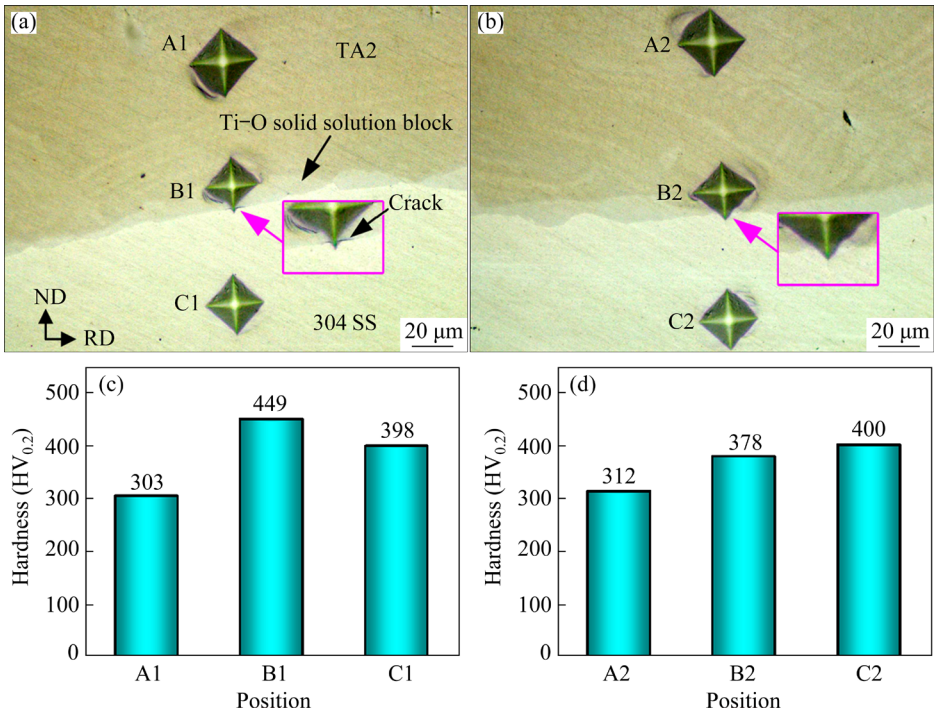

Fig. 4 Hardness of bond interface in cold rolled state: (a, c) With Ti−O solid solution block; (b, d) Without Ti−O solid solution block

the presence of Ti−O solid solution blocks. It is clear that the hardness of the Ti−O solid solution block at the titanium/stainless steel bond interface is over HV 146 and HV 51 greater than that of the titanium matrix and stainless steel matrix, respectively. Moreover, the indentation for hardness measurement leads to crack formation at the junction between the Ti−O solid solution block and the stainless steel. In contrast, the hardness at the interface devoid of a Ti−O solid solution block falls between the hardness values of the titanium matrix and the stainless steel matrix.

3.2 Structure and morphology of bond interface

Figure 5 shows the impact of annealing titanium plates and the thickness of the Ti−O solid solution layer on the morphology of the TSSLCP bond interface in its cold-rolled state. The titanium/stainless steel bond interface, whether with or without the Ti−O solid solution block, appears to be relatively flat. There is minimal interlocking between the titanium and stainless steel. During the cold roll bonding process, the Ti−O solid solution block does not deflect significantly and maintains approximately parallel distribution at interface. The presence of the Ti−O solid solution layer on the surface of titanium plate does not lead to the formation of a strong interfacial interlock at the bond interface.

Figure 6 illustrates the effects of annealing and grinding on the phase composition at the TSSLCP interface in its cold-rolled state. It is indicated that when the bonding surface of titanium plate is ground, preserving a certain thickness of Ti−O solid solution layer, the phases present at the cold roll-bonded titanium/stainless steel interface are α-Ti, α-Fe, and γ-Fe, corresponding to the fundamental phases of the titanium and stainless steel matrices. No oxides or other impurities are observed.

Figure 7 shows the SEM images of the bond interface with Ti−O solid solution blocks, obtained using various sampling methods. Specifically, Fig. 7(b) shows the application of the fixed-point polishing technique to the bond interface of the Ti−O solid solution block, using argon ion polishing. Figure 7(a) shows that after etching the bond interface with a titanium etchant, numerous voids form around the Ti−O solid solution blocks. However, the interface between the Ti−O solid solution blocks appears well bonded, with no voids.

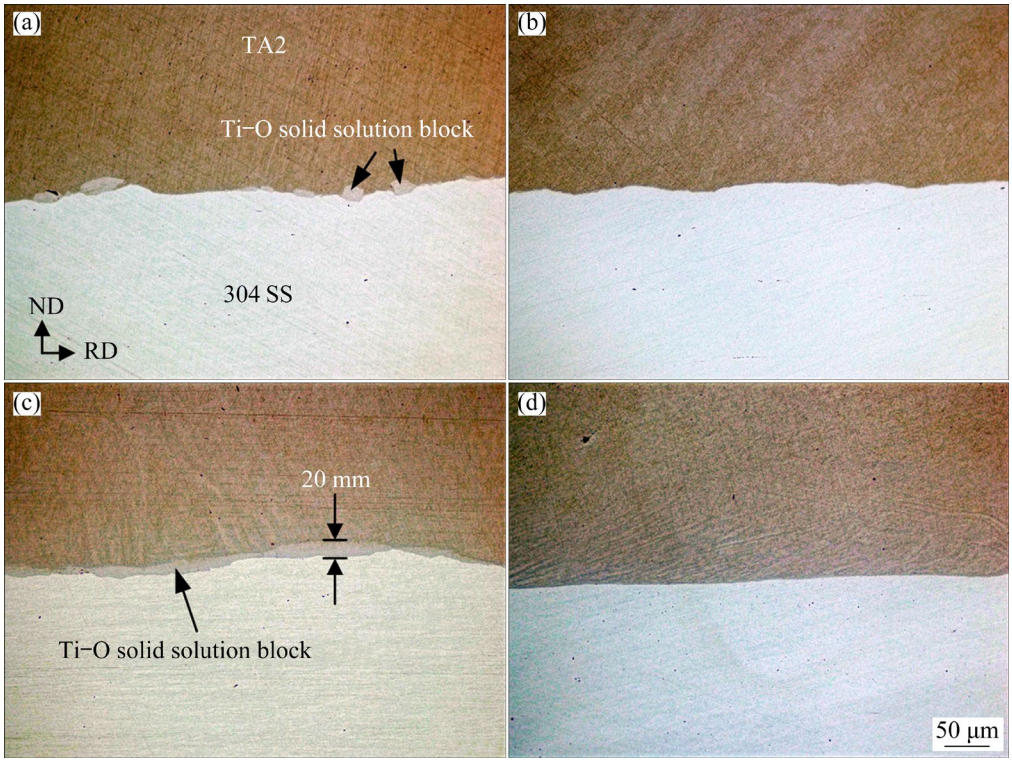

Fig. 5 Effect of annealing temperature of titanium plates and Ti−O solid solution layer on morphology of bond interface in cold rolled state: (a) 800 ℃, 10 μm-thick; (b) 800 ℃, no Ti−O solid solution block; (c) 1000 ℃, 20 μm-thick; (d) 1000 ℃, no Ti−O solid solution block

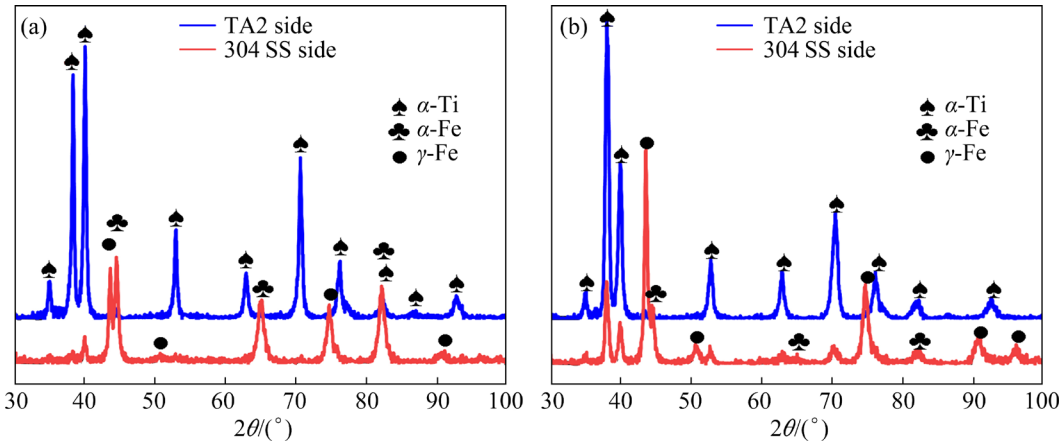

Fig. 6 Effect of annealing temperature of titanium plates and grinding on phase composition of bond interfaces in cold rolled state: (a) 800 ℃, 5 μm removed by grinding; (b) 1000 ℃, 5 μm removed by grinding

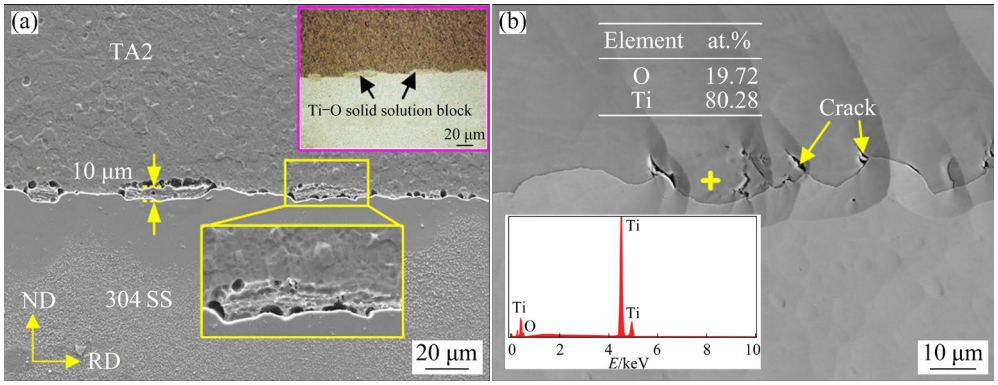

Fig. 7 SEM images of titanium/stainless steel bond interfaces containing Ti−O solid solution blocks: (a) Titanium etchant etching; (b) Argon ion polishing

Figure 7(b) reveals that the rupture of the Ti−O solid solution layer results in a multiscale fracture, with the fracture tip pointing towards the titanium side. Multi-scale fracture of the hardened layer has also been observed in other research [21]. Stainless steel can fill the larger fractures but struggles with the microcracks. Consequently, the bond interface exhibits a weak interlock morphology and a significant number of residual microcracks.

Figure 8 displays the microstructure of the TSSLCP bond interface, highlighting the presence of Ti−O solid solution blocks. Figure 8(a) shows a weak interlock between titanium and stainless steel at the bond interface, with cracks in the interlock teeth due to insufficient metal filling. Figures 8(b−e) show that the titanium near the interface has completely recrystallized, forming a fine equiaxed grain structure. Notably, the grain size of titanium in the interlock region is significantly smaller than that in other areas. For example, the average grain size of titanium in the interlock region (indicated by the orange dashed box) is 0.63 μm, while in the non-interlock region (designated by the green dashed box), it is 2.64 μm.

3.3 Morphology of tensile shear section of laminated composite plates

Figure 9 illustrates the effects of the annealing temperature of the titanium plates and the thickness of the Ti−O solid solution layer on the tensile shear fracture surface morphology of the cold-rolled TSSLCP.

Figure 9 shows a significant number of Ti−O solid solution blocks on the titanium side. These blocks display distinct grinding marks on their surfaces, with the edges of adjacent Ti−O solid solution blocks aligning with each other. Notably, with the annealing temperature of the titanium plate increasing from 800 to 1000 °C and the thickness of the Ti−O solid solution layer growing from 10 to

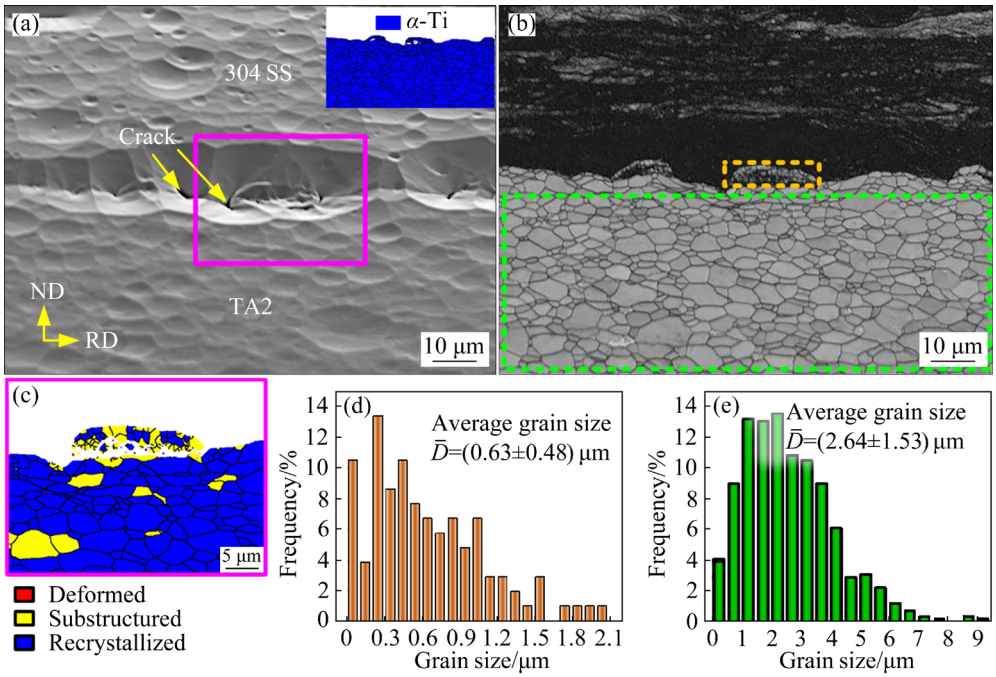

Fig. 8 Microstructure and morphology of bond interfaces containing Ti−O solid solution blocks: (a) SEM image; (b) Grain boundary and band contrast map; (c) Grain distribution map on titanium side; (d) Statistics of titanium grain size in orange dashed box; (e) Statistics of titanium grain size in green dashed box

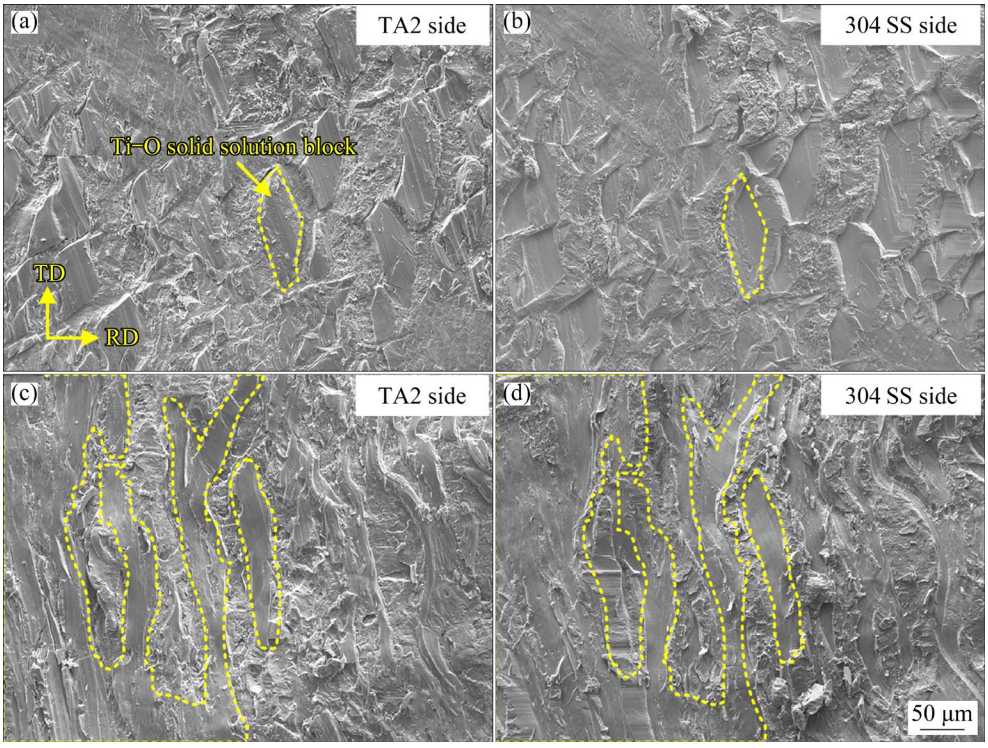

Fig. 9 Influence of annealing temperature of titanium plates and Ti−O solid solution layer on tensile-shear section morphology in cold rolled state: (a, b) 800 ℃, 10 μm-thick; (c, d) 1000 ℃, 20 μm-thick

20 μm, there is a corresponding increase in the size of the Ti−O solid solution blocks. On the stainless steel side, a considerable number of pits are observed in the section. The morphology, size, and distribution of these pits correspond to those of the Ti−O solid solution blocks on the titanium side.

Figure 10 shows the effect of the Ti−O solid solution layer thickness on the tensile-shear fracture morphology of TSSLCP at the bonding surface of the titanium plate. When the titanium plate surface has a 20 μm-thick Ti−O solid solution layer, the TSSLCP tensile-shear fracture tends to occur within this layer. On the stainless steel side, numerous discrete residual Ti−O solid solution particles are observed, showing brittle fracture along crystallographic planes. In contrast, when there is no Ti−O solid solution layer on the titanium plate surface, larger pieces of residual titanium are observed on the stainless steel side. These residual titanium pieces exhibit a shear-tough nest-like fracture morphology. In areas lacking the shear-tough nest morphology, numerous smaller residual titanium particles are observed, exhibiting a tough fracture with a ligamentous fossa morphology.

4 Discussion

As shown in Fig. 3, the interfacial bonding strength of TSSLCP is significantly correlated with the presence of Ti−O solid solution layer on the bonding surface of the titanium plate. Specifically, the highest interfacial bonding strength is observed in the absence of Ti−O solid solution layer. Conversely, the interfacial bonding strength decreases significantly when Ti−O solid solution layer is present, exceeding a reduction of 57 MPa. Furthermore, the hardness of the Ti−O solid solution layer is substantially higher than that of both the titanium matrix and the stainless steel matrix. This observation is in stark contrast to the introduction of a hardened layer on a steel plate's surface, which can lead to deep interlocking at the aluminum/steel bond interface [9]. Importantly, Fig. 6 shows that the bond interface with Ti−O solid solution blocks contains only the fundamental phases of titanium and stainless steel. This indicates that the bond interface is oxide-free and devoid of other impurities. Thus, the reduction in bond strength at the titanium/stainless steel interface can be solely attributed to the presence of the Ti−O solid solution layer.

Figure 7 shows multi-scale cracks forming at the locations of the Ti−O solid solution blocks at the bond interface. The stainless steel has difficulty flowing and filling the microcracks within these blocks, leading to numerous microcracks at the titanium/stainless steel bond interface. The high hardness and low plasticity of the Ti−O solid solution layer render it being prone to rupture during the cold roll bonding process. This rupture

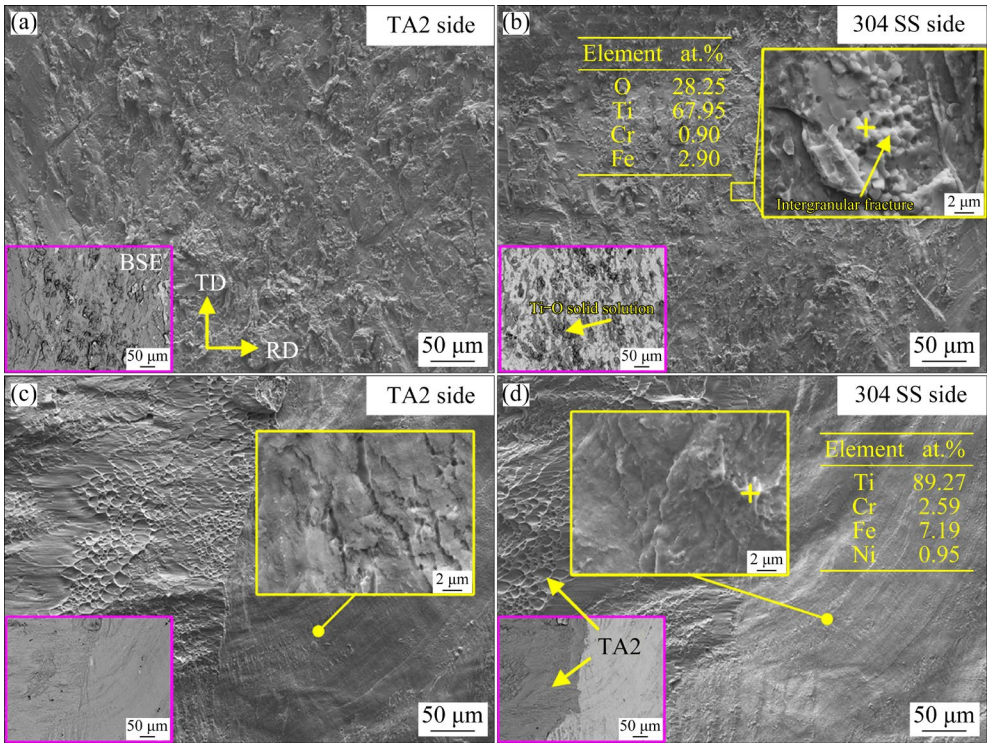

Fig. 10 Influence of Ti−O solid solution layer on morphology of tensile shear fracture surface: (a, b) 20 μm-thick Ti−O solid solution layer; (c, d) No Ti−O solid solution layer

exposes virgin metal and aids in the embedding of the component metals [22,23]. However, under the experimental conditions of this study, the Ti−O solid solution layer does not promote the formation of a strongly interlocked morphology at the cold-rolled bond interface. This can be attributed to the mechanical properties of stainless steel. Specifically, 304 stainless steel has a high strain hardening rate and resists localized deformation. This advantage ensures excellent homogeneous deformation in 304 stainless steel but complicates the generation of localized inhomogeneous deformation, making it more challenging to achieve [14,24].

During the cold roll bonding process, the extrusion filling of cracks involves local deformation, with the metal flowing strongly to fill the cracks in the hardened layer causing further crack expansion. This process ultimately aims to create a strongly interlocked morphology between the component metals. However, under the experimental conditions of this study, stainless steel exhibits a high work-hardening rate. This results in a rapid increase in the strength of the stainless steel deformed at the cracks within the Ti−O solid solution layer. Consequently, the difficulty for stainless steel to further flow and fill these cracks increases significantly. As a result, numerous microcracks form due to the rupture of the Ti−O solid solution layer, and these microcracks cannot be effectively filled or eliminated. The presence of these microcracks not only reduces the bonding rate at the interface but also acts as a source for cracks during deformation. This accelerates the failure of the bond interface, leading to a reduction in interfacial bonding strength [25,26].

Conventional cold roll bonded laminated metal composites, composed of titanium and metals with low work-hardening rates like aluminum [27] and carbon steel [28], are less likely to form microcracks at the bond interface. This is caused by the relatively low work-hardening rates of aluminum and carbon steel, as well as the ability to fill the hardened layer fractures on the titanium side during extrusion in cold roll bonding process. However, metals with high work-hardening rates pose a greater challenge for the cold roll bonding process to flow and fill the hardened layer cracks. This can result in insufficient filling of the hardened layer cracks, leading to the formation of cracks at the bond interface and a reduction in interfacial bond strength.

Figure 8 shows a weak interlock between titanium and stainless steel at the bond interface, while Fig. 9 reveals prominent Ti−O solid solution blocks in the tensile shear section on the titanium side, with a complementary indentation on the corresponding section of the stainless steel side. This indicates that the titanium embedded in the stainless steel side in Fig. 8 is a Ti−O solid solution block. By comparing with Fig. 5, it is clear that the Ti−O solid solution block is only shallowly embedded in the stainless steel, indicating a lack of deep interlocking. The Ti−O solid solution block is primarily distributed along the relatively straight bond interface. In Fig. 8, the grain size of titanium within the Ti−O solid solution block is significantly smaller than that in the surrounding areas, attributed to the solid solution of oxygen atoms. According to metal recrystallization theory, a hardened layer formed by work-hardening increases strain storage energy, so recrystallization and grain growth are expected to occur more rapidly during annealing [29,30]. However, the solid solution of oxygen atoms in titanium, forming a Ti−O solid solution, raises the recrystallization temperature of titanium and slows the grain growth rate, resulting in a finer grain structure [31].

Figure 10(a) shows that the presence of a Ti−O solid solution layer on the bonding surface of the titanium plate leads to a significant concentration of discrete residual Ti−O solid solution particles in the tensile shear section of the stainless steel side. This results in a brittle intercrystalline fracture morphology. The brittleness of the Ti−O solid solution is attributed to the influence of oxygen solutes, which alter the deformation mechanism of titanium [32].

Despite its fine-grained structure, the Ti−O solid solution does not enhance strength or toughness. The difficulty in achieving a strong interlock between titanium and stainless steel results in a relatively flat bond interface. Consequently, numerous hard and brittle Ti−O solid solution blocks are found distributed across this flat interface. This phenomenon is similar to the formation of numerous hard and brittle inter-metallic compounds at the bond interface, which compromises interfacial bonding strength [33]. These Ti−O solid solution blocks, distributed along

the flat interface, act as weak points, leading to a decrease in interfacial bonding strength. In contrast, when the titanium plate surface is devoid of a Ti−O solid solution layer, the tensile shear section on stainless steel side shows a tougher and more ductile fracture morphology, as shown in Fig. 10(b). This suggests that the absence of a Ti−O solid solution enhances interfacial bonding strength. In summary, when deep interlocking between the component metals is challenging to achieve, the presence of hard and brittle hardened blocks at the flat bond interface can significantly reduce interfacial bonding strength.

Figure 11 shows the formation mechanism of the cold roll bonded TSSLCP interface microstructure when there is a Ti−O solid solution layer on the bonding surface of the titanium plate. During the cold roll bonding process, the Ti−O solid solution layer on the titanium plate ruptures, creating Ti−O solid solution blocks and multi-scale cracks. The stainless steel's ability to extrude and fill these cracks within the Ti−O solid solution layer is limited, resulting in a large number of microcracks at the bond interface. Consequently, achieving a deep interlock morphology at the bond interface becomes difficult, leading to the distribution of Ti−O solid solution blocks along an approximately straight bond interface.

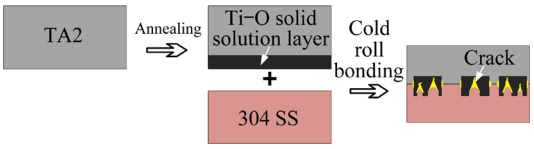

Fig. 11 Formation mechanism of interfacial microstructure of cold roll bonded TSSLCP

5 Conclusions

(1) The presence of the Ti−O solid solution layer reduces the interfacial bonding strength of the titanium/stainless steel laminated composite plate from over 261 MPa to below 204 MPa.

(2) Rupture of the Ti−O solid solution layer during the cold roll-bonding process generates multi-scale cracks, and the limited ability of stainless steel to fill these cracks results in numerous microcracks at the bond interface.

(3) The difficulty for stainless steel to fill the cracks in the Ti−O solid solution layer hinders the formation of deep interlocking between titanium and stainless steel. The Ti−O solid solution blocks tend to distribute along the nearly flat bonding interface, making them prone to preferential fracture during deformation.

(4) During the cold roll-bonding process, it is difficult to promote the formation of deep interlocking interfaces and improve the binding strength by constructing a hardened layer when the component metals possess a high work-hardening rate.

CRediT authorship contribution statement

Zhi-yan YANG: Methodology, Visualization, Conceptualization, Writing – Original draft; **Xue-feng LIU:** Funding acquisition, Conceptualization, Writing − Reviewing & editing; **Hong-ting CHEN:** Writing − Reviewing & editing; **Xin MA:** Writing − Reviewing & editing.

Declaration of competing interest

The authors declare that they have no known competing financial interests or personal relationships that could have appeared to influence the work reported in this paper.

Acknowledgments

This work was supported by the National Key R&D Program of China (No. 2018YFA0707300), the National Natural Science Foundation of China (No. 52374376), and the Introduction Plan for High end Foreign Experts, China (No. G2023105001L).

References

[1] TAYYEBI M, RAHMATABADI D, KARIMI A, ADHAMI M, HASHEMI R. Investigation of annealing treatment on the interfacial and mechanical properties of Al5052/Cu multilayered composites subjected to ARB process [J]. Journal of Alloys and Compounds, 2021, 871: 159513.

[2] GHOLAMI M D, HASHEMI R, SEDIGHI M. The effect of temperature on the mechanical properties and forming limit diagram of aluminum strips fabricated by accumulative roll bonding process [J]. Journal of Materials Research and Technology, 2020, 9: 1831−1846.

[3] TAYYEBI M, ADHAMI M, KARIMI A, RAHMATABADI D, ALIZADEH M, HASHEMI R. Effects of strain accumulation and annealing on interfacial microstructure and grain structure (Mg and Al_3Mg_2 layers) of Al/Cu/Mg multilayered composite fabricated by ARB process [J]. Journal of Materials Research and Technology, 2021, 14: 392−406.

[4] GAO Hai-tao, KONG C, YU Hai-liang. Lightweight metal laminated plates produced via (hot, cold and cryogenic) roll

bonding: A review [J]. Transactions of Nonferrous Metals Society of China, 2023, 33(2): 337−356.

[5] KIM H J, HONG S I. Effect of Ni interlayer on the interface toughening and thermal stability of Cu/Al/Cu clad composites [J]. Metals and Materials International, 2019, 25(1): 94−104.

[6] FU Lun, XIAO Hong, YU Chao, CHEN Nan, GUO Yuan-chang, YANG Bin, REN Zhong-kai. Analysis on mechanism of steel plate pre-oxidation in improving bonding properties of cold-rolled 6061 Al/Q235 steel composite plate [J]. Journal of Materials Processing Technology, 2023, 316: 117960.

[7] HUO Peng-da, LI Feng, WANG Ye, LI Chao. Corrugated interface structure and formation mechanism of Al/Mg/Al laminate rolled by hard plate [J]. Transactions of Nonferrous Metals Society of China, 2023, 33(4): 1038−1053.

[8] BAY N. Mechanisms producing metallic bonds in cold welding [J]. Welding Journal, 1983, 62(5): 137−142.

[9] WU Bo, LI Long, XIA Cheng-dong, GUO Xiao-feng, ZHOU De-jing. Effect of surface nitriding treatment in a steel plate on the interfacial bonding strength of the aluminum/steel clad sheets by the cold roll bonding process [J]. Materials Science and Engineering A, 2017, 682: 270−278.

[10] FAKHER S, REIHANIAN M, LARI BAGHAL S M, FATAHI L. Role of cracked interlayer on deformation processing of Al/hard chrome/Al laminate [J]. Metals and Materials International, 2021, 27: 4780−4792.

[11] LIU Zhu-bo, WANG Xin-yue, LIU Ming-shuo, LIU Yuan-ming, LIU Jiang-lin, IGNATOV A V, WANG Tao. Microstructure and mechanical behavior of Ti/Cu/Ti laminated composites produced by corrugated and flat rolling [J]. Transactions of Nonferrous Metals Society of China, 2022, 32(8): 2598−2608.

[12] REN Zhong-kai, GUO Xiong-wei, LIU Xiao, MA Xiao-bao, JIANG Shu-yong, BIAN Li-ping, WANG Tao, HUANG Qing-xue. Effect of pulse current treatment on interface structure and mechanical behavior of TA1/304 clad plates [J]. Materials Science and Engineering A, 2022, 850: 143583.

[13] CHEN Xiang, INAO D, TANAKA S, LI Xiao-jie, BATAEV I A, HOKAMOTO K. Comparison of explosive welding of pure titanium/SUS 304 austenitic stainless steel and pure titanium/SUS 821L1 duplex stainless steel [J]. Transactions of Nonferrous Metals Society of China, 2021, 31(9): 2687−2702.

[14] KISHORE K, KUMAR R G, CHANDAN A K. Critical assessment of the strain-rate dependent work hardening behaviour of AISI 304 stainless steel [J]. Materials Science and Engineering A, 2021, 803: 140675.

[15] ZHANG Hong-wang, ZHAO Yi-ming, WANG Yu-hui, YU Hua-xin, ZHANG Chun-ling. Fabrication of nanostructure in inner-surface of AISI 304 stainless steel pipe with surface plastic deformation [J]. Journal of Materials Science & Technology, 2018, 34(11): 2125−2130.

[16] CONRADIE F, TREURNICHT N, SACKS N. Alpha case characterization of hot rolled titanium [J]. Advanced Materials Research, 2014, 1019: 311−317.

[17] DESHMUKH V, KADAM R, JOSHI S S. Removal of alpha case on titanium alloy surfaces using chemical milling [J]. Machining Science and Technology, 2017, 21(2): 257−278.

[18] FUKAI H, IIZUMI H, MINAKAWA K, OUCHI C. The effects of the oxygen-enriched surface layer on mechanical properties of α+β type titanium alloys [J]. ISIJ International, 2005, 45(1): 133−141.

[19] DZIALLACH S, BLECK W, KÖHLER M. Roll-bonded titanium/stainless-steel couples. Part 3: Adhesion properties [J]. Advanced Engineering Materials, 2010, 12(9): 848−854.

[20] HOSEINI M, HAMID POURIAN M, BRIDIER F, VALI H, SZPUNAR J A, BOCHER P. Thermal stability and annealing behaviour of ultrafine grained commercially pure titanium [J]. Materials Science and Engineering A, 2012, 532: 58−63.

[21] BAI Yu-liang, LIU Xue-feng, SHI Zhang-zhi. Stress-induced alternating microstructures of titanium/steel bonding interface [J]. Materials Letters, 2021, 298: 130019.

[22] JIANG Yong, MAO Hai-rong, WANG Xiao-wei, LU Yi-lan, GONG Jian-ming. Effect of oxygen boost diffusion treatment on the mechanical properties of Ti−6Al−4V alloy [J]. Surfaces and Interfaces, 2021, 25: 101248.

[23] JAFFEE R I, CAMPBELL I E. The effect of oxygen, nitrogen, and hydrogen on iodide refined titanium [J]. The Journal of the Minerals, Metals & Materials Society, 1949, 1(9): 646−654.

[24] MAKKOUK R, BOURGEOIS N, SERRI J, BOLLE B, MARTINY M, TEACA M, FERRON G. Experimental and theoretical analysis of the limits to ductility of type 304 stainless steel sheet [J]. European Journal of Mechanics-A/Solids, 2008, 27(2): 181−194.

[25] WANG Chun-yang, JIANG Yan-bin, XIE Jian-xin, ZHOU De-jing, ZHANG Xiao-jun. Effect of the steel sheet surface hardening state on interfacial bonding strength of embedded aluminum-steel composite sheet produced by cold roll bonding process [J]. Materials Science and Engineering A, 2016, 652: 51−58.

[26] GAO Chuang, LI Long, CHEN Xin, ZHOU De-jing, TANG Chao-lan. The effect of surface preparation on the bond strength of Al-St strips in CRB process [J]. Materials & Design, 2016, 107: 205−211.

[27] LIU Jia-geng, WU Jiang, LIU Qian, JI Shuai, ZHENG Xin-lu, WANG Feng, WANG Jiang. Effect of the strength of initial aluminium on the bonding properties and deformation coordination of Ti/Al composite sheets by the cold roll bonding process [J]. Crystals, 2022, 12(11): 1665.

[28] BAI Yu-liang, LIU Xue-feng. Interfacial reaction behavior of titanium/steel composite plate formed by cold-hot rolling [J]. Materials Characterization, 2023, 202: 113030.

[29] LOPEZ-SANCHEZ M A, TOMMASI A, BAROU F, QUEY R. Dislocation-driven recrystallization in AZ31B magnesium alloy imaged by quasi-in situ EBSD in annealing experiments [J]. Materials Characterization, 2020, 165: 110382.

[30] BURKE J E, TURNBULL D. Recrystallization and grain growth [J]. Progress in Materials Science, 1952, 3: 220−292.

[31] OUCHI C, IIZUMI H, MITAO S. Effects of ultra-high purification and addition of interstitial elements on properties of pure titanium and titanium alloy [J]. Materials Science and

Engineering A, 1998, 243: 186−195.
[32] CHONG Yan, POSCHMANN M, ZHANG Ruo-peng, ZHAO Shi-teng, HOOSHMAND M S, ROTHCHILD E, OLMSTED D L, MORRIS JR. J W, CHRZAN D C, ASTA M, MINOR A M. Mechanistic basis of oxygen sensitivity in titanium [J]. Science Advances, 2020, 6(43): eabc4060.
[33] WANG Qian, LENG Xue-song, YANG Tian-hao, YAN Jiu-chun. Effects of Fe−Al intermetallic compounds on interfacial bonding of clad materials [J]. Transactions of Nonferrous Metals Society of China, 2014, 24(1): 279−284.

Ti−O 固溶体层对钛/不锈钢冷轧复合板界面结合强度的影响及机理

杨智研[1,2,3]，刘雪峰[1,2,3]，陈虹廷[1,2,3]，马 欣[1,4]

1. 北京科技大学 北京材料基因工程高精尖创新中心，北京 100083；
2. 北京科技大学 现代交通金属材料与加工技术北京实验室，北京 100083；
3. 北京科技大学 材料先进制备技术教育部重点实验室，北京 100083；
4. 新疆工程学院 机电工程学院，乌鲁木齐 830023

摘 要：将以 Ti−O 固溶体层作为待复合表面硬化层的钛板与具有高加工硬化率的 304 不锈钢板进行冷轧复合，研究了界面结合强度的变化规律及影响机理。结果表明，硬化层导致钛/不锈钢复合板的界面结合强度从 261 MPa 以上降低至 204 MPa 以下。硬化层在冷轧复合过程中破裂形成多尺度裂口，不锈钢难以填充硬化层裂口，不仅影响互锁界面的形成，而且导致复合界面形成大量微裂纹和沿近似平直界面分布的硬化块，降低界面结合强度。当组元金属具有高加工硬化率时，常规通过构建表面硬化层以增强界面互锁并提高界面结合强度的策略难以起效。

关键词：钛/不锈钢复合板；Ti−O 固溶体硬化层；互锁界面形成机理；界面结合强度

(Edited by Bing YANG)